DEUTSCHES ELEKTRONEN – SYNCHROTRON

DESY 93-008
March 1993

Radiative Corrections to $e^+e^- \to Zh^0$ and $Z \to \nu\bar{\nu}h^0$ in the Minimal Supersymmetric Model

A. Hemptinne

Deutsches Elektronen-Synchrotron DESY, Hamburg

B. Kniehl

II. Institut für Theoretische Physik, Universität Hamburg

ISSN 0418-9833

NOTKESTRASSE 85 – D-2000 HAMBURG 52

DESY 93-033
March 1993

ISSN 0418-9833

Radiative Corrections to $e^+e^- \to Zh^0$ and $Z \to \gamma h^0$ in the Minimal Supersymmetric Model

RALF HEMPFLING

Deutsches Elektronen-Synchrotron, Notkestraße 85, W-2000 Hamburg 52, Germany

BERND KNIEHL

II. Institut für Theoretische Physik, Universität Hamburg, W-2000 Hamburg 50, Germany*

ABSTRACT

The Higgs sector of the minimal supersymmetric extension of the standard model (MSSM) becomes phenomenologically hard to distinguish from the standard model (SM) in the limit that the CP-odd scalar, A^0, is much heavier than the Z boson. If, in addition, all the superpartners lie outside the kinematic reach of present-day (or near-future) colliders the only experimental evidence for supersymmetry (SUSY) might be through internal loops involving superpartners. We have calculated sfermion-induced radiative corrections to $e^+e^- \to Zh^0$ and $Z \to \gamma h^0$ in the MSSM, which are enhanced for high m_t.

* *Supported by the Bundesministerium für Forschung und Technologie, 05 5 HH 91P(8), Bonn, Germany*

1. Introduction

The SM of the electroweak and strong interactions is in excellent agreement with all presently observed phenomena at the electroweak scale. Nonetheless, there are a number of theoretical shortcomings. Perhaps the most puzzling problem is to explain the origin (and stability) of the large hierarchy between the Planck scale (10^{19} GeV) and the scale of electroweak symmetry breaking [1]. SUSY is to date the most promising attempt to try and solve this problem and still retain the Higgs fields as fundamental scalars. In supersymmetric theories, quadratic divergences in unrenormalized Green functions are automatically cancelled by adding to every fermion (boson) a bosonic (fermionic) partner with the same quantum numbers and imposing SUSY on the resulting Lagrangian. While the exact origin of the electroweak scale in SUSY is still unclear, the cancellation of quadratic divergences readily explains the stability of the electroweak scale (or any other intermediate scale) under radiative corrections.

In the minimal supersymmetric extension of the Standard Model (MSSM), one simply adds a supersymmetric partner to every quark, lepton, and gauge boson. In addition, the MSSM must possess two Higgs doublets (H_1 and H_2) in order to give masses to up- and down-type fermions in a manner consistent with supersymmetry and to avoid gauge anomalies introduced by the fermionic superpartners of the Higgs bosons. In this model SUSY is broken by adding explicit soft SUSY breaking terms to the theory. With these terms the vacuum expectation values of the Higgs fields, $v_i \equiv \langle H_i \rangle$, can become non-zero and the electroweak gauge symmetry can be broken spontaneously. Then the Higgs sector of the MSSM possesses five physical Higgs states: a charged Higgs pair ($H^\pm$), a CP-odd Higgs scalar (A^0) and two CP-even Higgs scalars (h^0 and H^0, with $m_{h^0} \leq m_{H^0}$) [3].

The h^0 [H^0] production rate is governed by the ZZh^0 [ZZH^0] vertex, which is suppressed relative to the SM by a factor of $\sin^2(\beta-\alpha)$ [$\cos^2(\beta-\alpha)$]. Here $(\beta-\alpha)$ is the angle between the direction of the vacuum expectation value and the H^0 eigenstate. In the MSSM this suppression factor can be expressed in terms of two physical input parameters, which we choose to be m_{h^0} and m_{A^0},

$$\cos^2(\beta-\alpha) = \frac{m_{h^0}^2(m_Z^2 - m_{h^0}^2)}{m_{A^0}^2(m_{A^0}^2 + m_Z^2 - 2m_{h^0}^2)}\,. \qquad (1.1)$$

In general, (1.1) has two solutions corresponding to $\tan\beta < 1$ and $\tan\beta > 1$. This ambiguity can be avoided temporarily by parameterizing the Higgs sector by $\tan\beta$ instead of m_{h^0}. However, $\tan\beta$ does not correspond to a physical observable and the ambiguity returns if one expresses $\tan\beta$ in terms of physical quantities.

It has been shown recently that radiative corrections to the lightest Higgs boson mass of the MSSM are very substantial [4]. Radiative corrections to vertices have also been computed using a renormalization group approach [5], an effective potential formalism [6], and the conventional one-loop calculus [7,8]. In Fig. 1, we show contours

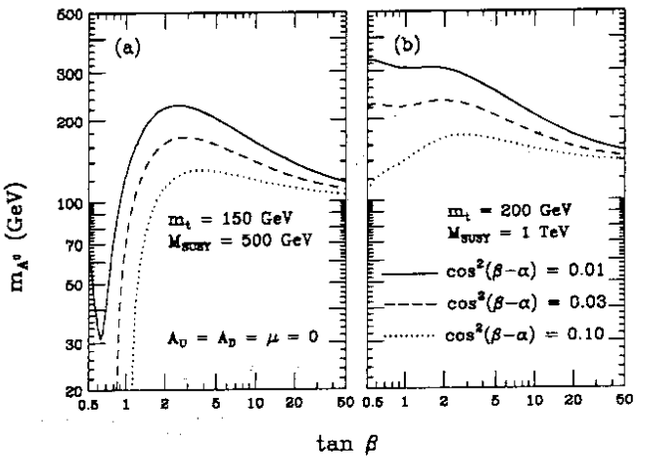

Fig. 1. Contours of constant $\cos^2(\beta-\alpha)$ in the $(\tan\beta, m_{A^0})$ plane. All the soft SUSY breaking mass parameters are taken to be 500 GeV (a) and 1 TeV (b) and we take $m_t = 150$ (a) and 200 GeV (b). Squark mixing is neglected (i.e. $A_U = A_D = \mu = 0$)

of constant $\cos^2(\beta-\alpha)$ in the $(\tan\beta, m_{A^0})$ plane. This plot includes the leading logarithmic corrections (i.e. terms that grow logarithmically with the scale of SUSY breaking, $M_{\rm SUSY}$) summed to all orders in perturbation theory [9]. We see that already for $m_{A^0} > 300$ GeV the deviation of the MSSM from the SM is only of the order of 1%.

The renormalization group approach and the effective potential approach are inadequate to calculate Higgs production rates in the case of $\sqrt{s} \gg m_Z$, where $\sqrt{s}$ is the centre-of-mass (CM) energy, since these formalisms require that $\mathcal{A}(p^2) \sim \mathcal{A}(m_Z)$ and $\mathcal{A}(p^2) \sim \mathcal{A}(0)$, respectively, where $\mathcal{A}$ is a generic renormalized Green function and p stands for some external four-momentum. Thus, our approach will be to combine the renormalization group approach and a full one-loop calculation done in the case where the second Higgs doublet is kinematically unaccessible, i.e., for $m_{A^0} > \sqrt{s}/2$ and thus $\cos(\beta-\alpha) \propto m_Z^2/m_{A^0}^2 \approx 0$; see (1.1) and Fig. 1.

This paper is organized as follows: In Sec. 2, we present our one-loop results. Their phenomenological implications are discussed in Sec. 3. Section 4 contains a summary and some concluding remarks. A complete set of Feynman rules is listed in Appendix A. The relevant unrenormalized one-loop Green functions are given in Appendix B.

2. One-loop radiative corrections

We will now proceed to calculate non-leading log radiative corrections in the limit of large m_{A^0}. In this limit, we are left with one Higgs boson, with SM couplings to matter fields and gauge bosons. The only difference to the SM will be the existence of additional $\mathrm{SU(2)_L \times U(1)_Y}$ representations (sfermions, gauginos, and higgsinos), which will enter the calculation through loops. (In addition, the allowed range of m_{h^0} is constrained by SUSY.) Thus we can immediately apply the SM renormalization scheme [10].

Our technical procedure is similar to [11,12]. We reduce the loop amplitudes to standard integrals [13] by means of the reduction algorithm of [14] and identify the ultraviolet divergencies by means of dimensional regularization [15]. We essentially work in the electroweak on-mass-shell (OMS) scheme [10], which uses the fine-structure constant, $\alpha_{\rm em}$, and the physical particle masses as basic parameters. However, we parameterize the lowest-order expressions in terms of the Fermi constant, G_F, rather than $\alpha_{\rm em}$. In turn, the quantity Δr appears in the radiative corrections in such a way that all would-be mass singularities associated with light charged fermions are removed. This procedure is sometimes called the modified on-mass-shell (MOMS) scheme [11,12]. We shall largely adopt the conventions of [10] and frequently use the short-hand notations

$$c_{\rm w}^2 = 1 - s_{\rm w}^2 = \frac{w}{z}\,, \quad w = m_W^2\,, \quad z = m_Z^2\,, \quad h = m_{h^0}^2\,. \quad (2.1)$$

The parameters and Feynman rules of the sfermion sector are explained in Appendix A.

To start with, we calculate the quantum corrections to the differential cross section of $e^+e^- \to Zh^0$ due to MSSM sfermions. These corrections comprise all additional m_t-dependent terms generated by the supersymmetric extension. At the one-loop level we neglect terms suppressed by $\cos(\beta-\alpha)$. The tree-level deviation from the SM due to non-zero values of $\cos(\beta-\alpha)$ can be included by multiplying the SM amplitude by a factor $\sin(\beta-\alpha)$. Leading-logarithmic corrections are accommodated by evaluating $\sin(\beta-\alpha)$ within the renormalization-group formalism [5]. Calling the angle between the e^- and Z-boson flight directions in the CM frame θ, we find

$$\frac{{\rm d}\sigma^{(Zh^0)}_{\rm MSSM}}{{\rm d}\cos\theta} = \frac{{\rm d}\sigma^{(Zh^0)}_{\rm SM}}{{\rm d}\cos\theta}\sin^2(\beta-\alpha)_{\rm LL}\left[1 + 2\,\mathcal{R}e\,\delta_{\widetilde{Q}} - 2\Delta r_{\widetilde{Q}} + \mathcal{O}\big(\alpha_{\rm em}\cos(\beta-\alpha)\big)\right], \quad (2.2)$$

where the subscript LL refers to the leading-log resummation. Here ${\rm d}\sigma^{(Zh^0)}_{\rm SM}/{\rm d}\cos\theta$ the is one-loop corrected SM prediction in the MOMS scheme, which may be found in [12]. The sfermion loop corrections to the $e^+e^- \to Zh^0$ amplitude (in the OMS scheme) are given by

$$\delta_{\widetilde{Q}} = \tfrac{1}{2}\,\mathcal{R}e\,\hat{A}'_{ZZ}(z) + \frac{\hat{A}_{ZZ}(s)}{s-z} + \frac{\Gamma^1_{h^0ZZ} - \delta\Gamma_{h^0ZZ} + F(\theta)\Gamma^4_{h^0ZZ}}{\Gamma^0_{h^0ZZ}} + \frac{v_e e_e}{v_e^2+a_e^2}\left[\frac{\hat{A}_{\gamma Z}(s)}{s} + \frac{s-z}{s}\,\frac{\Gamma^1_{h^0\gamma Z} + F(\theta)\Gamma^4_{h^0\gamma Z}}{\Gamma^0_{h^0ZZ}}\right], \quad (2.3)$$

where $v_e = (T_3^e - 2s_{\rm w}^2 e_e)/(2c_{\rm w}s_{\rm w})$, $a_e = T_3^e/(2c_{\rm w}s_{\rm w})$, $\Gamma^0_{h^0ZZ} = em_Z/(c_{\rm w}s_{\rm w})$, and

$$F(\theta) = \frac{(h-z-s)\lambda\sin^2\theta}{2(8zs+\lambda\sin^2\theta)}\,, \quad (2.4)$$

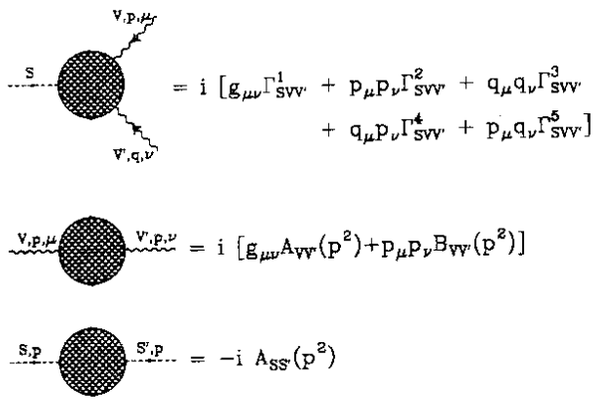

Fig. 2. Lorentz-invariant decomposition of the one-particle irreducible Green functions. Here S and S' stand for scalar particles (in our case h^0) and V, V' stand for vector bosons (in our case γ and Z)

with $\lambda = s^2+z^2+h^2-2(sz+zh+hs)$, contains the angular dependence. The unrenormalized sfermion contributions to the (transverse) boson vacuum polarizations, A_{WW}, A_{ZZ}, $A_{\gamma Z}$, $A_{\gamma\gamma}$, and $A_{h^0h^0}$, and the relevant h^0ZZ and $h^0\gamma Z$ form factors, $\Gamma^{1,4}_{h^0ZZ}$ and $\Gamma^{1,4}_{h^0\gamma Z}$, are listed in Appendix B. Our conventions are explained in Fig. 2. The renormalized ZZ and γZ vacuum polarizations are given by

$$\hat{A}_{ZZ}(s) = A_{ZZ}(s) - \mathcal{R}e\,A_{ZZ}(z) + (s-z)\left[\left(\frac{c_{\rm w}^2}{s_{\rm w}^2}-1\right)X - A'_{\gamma\gamma}(0)\right], \quad (2.5)$$
$$\hat{A}_{\gamma Z}(s) = A_{\gamma Z}(s) + s\frac{c_{\rm w}}{s_{\rm w}}X\,,$$

where

$$X = \mathcal{R}e\left(\frac{A_{WW}(w)}{w} - \frac{A_{ZZ}(z)}{z}\right). \quad (2.6)$$

The h^0ZZ counterterm reads

$$\frac{\delta\Gamma^1_{h^0ZZ}}{\Gamma^0_{h^0ZZ}} = \tfrac{1}{2}\,\mathcal{R}e\left[-\left(\frac{c_{\rm w}^2}{s_{\rm w}^2}-1\right)\frac{A_{WW}(w)}{w} + \frac{c_{\rm w}^2}{s_{\rm w}^2}\,\frac{A_{ZZ}(z)}{z} - A'_{h^0h^0}(h)\right] - \tfrac{1}{2}A'_{\gamma\gamma}(0)\,. \quad (2.7)$$

The sfermionic corrections to the muon lifetime are

$$\Delta r_{\widetilde{Q}} = \frac{\mathcal{R}e\,A_{WW}(w) - A_{WW}(0)}{w} + \frac{c_{\rm w}^2}{s_{\rm w}^2}\,\mathcal{R}e\left(\frac{A_{ZZ}(z)}{z} - \frac{A_{WW}(w)}{w}\right) - A'_{\gamma\gamma}(0)\,. \quad (2.8)$$

Note that the terms contained within the square brackets of Eq. (2.2) do not contain leading logarithms, so that there is no problem with double counting. Virtual sfermions occur also in the selectron-neutralino and sneutrino-chargino loops contributing to the electron self-energy and the $e^+e^-\phi$ vertex corrections ($\phi = h^0, Z, \gamma$). However, these types of corrections do not involve a summation over the generations and are independent of m_t. We thus expect them to be negligible.

Equation (2.2) can be integrated easily to give the total cross section of $e^+e^- \to Zh^0$,

$$\sigma_{\rm MSSM}^{(Zh^0)} = \sigma_{\rm SM}^{(Zh^0)} \sin^2(\beta-\alpha)_{\rm LL} \left[1 + 2\,\mathcal{R}e\,\Delta_{\widetilde{Q}} - 2\Delta r_{\widetilde{Q}} + \mathcal{O}(\alpha_{\rm em}\cos(\beta-\alpha))\right], \tag{2.9}$$

where $\Delta_{\widetilde{Q}} = \delta_{\widetilde{Q}}|_{\theta=\pi/3}$ and $\sigma_{\rm SM}^{(Zh^0)}$ is the one-loop corrected SM result in the MOMS scheme [12].

The process $e^+e^- \to \mu^+\mu^-$ has a particularly clear signature and is being extensively studied at LEP and SLC. It lends itself to a reference process for experiments at future e^+e^- colliders at higher energies, too, since dimuons will be identified easily. Clearly, the ratio $R = \sigma(e^+e^- \to Zh^0)/\sigma(e^+e^- \to \mu^+\mu^-)$ can be measured more accurately than its numerator and denominator separately because uncertainties in the absolute luminosity calibration cancel. To predict how R is affected by the presence of sfermions, we need to also calculate their loop contributions to the $e^+e^- \to \mu^+\mu^-$ cross section. Since sfermion loops do not occur in vertex and box amplitudes in this case, we can resort to the improved Born approximation [16] and write

$$\sigma_{\rm MSSM}^{(\mu^+\mu^-)} = \tfrac{3}{4}\pi\alpha_{\rm em}^2 s \left\{ \frac{\left(|\bar{v}_e|^2 + a_e^2\right)\left(|\bar{v}_\mu|^2 + a_\mu^2\right)}{\left|s - z - \hat{A}_{ZZ}(s)\right|^2} + 2\,\mathcal{R}e\,\frac{\bar{v}_e e_e \bar{v}_\mu e_\mu}{\left(s - z - \hat{A}_{ZZ}(s)\right)\left(s - \hat{A}_{\gamma\gamma}(s)\right)^*} + \frac{e_e^2 e_\mu^2}{\left|s - \hat{A}_{\gamma\gamma}(s)\right|^2} \right\}, \tag{2.10}$$

where $\bar{v}_f = \left(T_3^f - 2\bar{s}_{\rm w}^2 e_f\right)/(2c_{\rm w}s_{\rm w})$, $\bar{s}_{\rm w}^2 = s_{\rm w}^2 + c_{\rm w}s_{\rm w} \times \hat{A}_{\gamma Z}(s)/s$ refers to the effective weak mixing angle appropriate to the $Zf\bar{f}$ coupling [16], $\hat{A}_{ZZ}$ and $\hat{A}_{\gamma Z}$ are defined by (2.5), and

$$\hat{A}_{\gamma\gamma}(s) = A_{\gamma\gamma}(s) - sA'_{\gamma\gamma}(0) \tag{2.11}$$

is the renormalized transverse photon self-energy. Since, for the time being, we aim at analyzing the deviation of R from its SM value, we need not include SM radiative corrections in (2.9) and (2.10). Moreover, it is not necessary to use the MOMS scheme here, since Δr cancels out in the ratio.

So far, we have considered the sfermionic corrections to Zh^0 associated production which will be the major source of h^0 bosons at future e^+e^- colliders with energy up to some 500 GeV. Presently, the h^0 boson is being looked for in the decay products of Z bosons on resonance. The Bjorken process [17], $Z \to Z^*h^0 \to f\bar{f}h^0$, is the dominant h^0-boson production mechanism for $m_{h^0} \lesssim 75$ GeV. For higher values of m_{h^0}, the $Z \to \gamma h^0$ decay mode which, proceeds in the SM through W-boson and heavy-fermion loops, dominates. SM radiative corrections to the Bjorken process were investigated in [18] and found to be typically of the order of 1%. Since the sfermionic contributions to the Zh^0 associated production are modest (see Sec. 3), we expect them to be truly negligible in the case of the Bjorken process, which emerges by crossing. However, this might be very different in the case of $Z \to \gamma h^0$, since here sfermions contribute already in lowest order.

We recall that the SM prediction for the $Z \to \gamma h^0$ decay rate reads [19]

$$\Gamma(Z \to \gamma h^0) = \frac{G_F m_Z^3}{3\pi\sqrt{2}} \left(1 - \frac{h}{z}\right) \left|\hat{E}_{ZAH}(z,0,h)\right|^2, \tag{2.12}$$

where $\hat{E}_{ZAH}$ is given in (2.10) of [12]. The sfermionic contributions may be incorporated by including the term $-\Gamma^1_{h^0\gamma Z}/\Gamma^0_{h^0 ZZ}$ within the absolute signs of (2.12); here the minus sign is needed to adapt the Feynman rules of the present paper to the slightly different conventions used in [12]. In the next section we shall see that the sfermion loops interfere destructively with the SM amplitudes so as to reduce the $Z \to \gamma h^0$ decay rate by several percent as compared to the SM prediction.

3. Numerical results

In this section we explore the phenomenological implications of our results. Our SM input parameters are adopted from [20], except for $m_Z = 91.187$ GeV [21] and the light-quark masses, which we take from [22]. Unless stated otherwise, we consider e^+e^- CM energy $\sqrt{s} = 300$ GeV and assume $m_t = 150$ GeV. Our MSSM reference values are $\mu = 200$ GeV and $A_U = A_D = M_{\widetilde{U}} = M_{\widetilde{D}} = M_{\widetilde{Q}} = 200$ GeV for all three generations of squarks and sleptons. In the large-m_{A^0} limit we obtain $\tan\beta$, which enters the calculation at the one-loop level, by solving the improved tree-level relation

$$\cos^2(2\beta) = \frac{m_{h^0}^2}{m_Z^2} - \frac{3G_F m_t^4}{\pi^2\sqrt{2}m_Z^2} \ln\frac{M_{\tilde{t}_1}M_{\tilde{t}_2}}{m_t^2}. \tag{3.1}$$

In our analysis we always require that $0.5 < \tan\beta < m_t/m_b$ and that all sfermions have masses larger than $m_Z/2$, in compliance with their nondiscovery at LEP and SLC.

Our final results are presented in Figs. 3–12. In Figs. 3–6, we investigate in turn the dependence of the sfermionic corrections, $2\,\mathcal{R}e\,\Delta_{\widetilde{Q}}$, to $\sigma(e^+e^- \to Zh^0)$ (in the OMS scheme) on m_t, $A_U = A_D$, $M_{\widetilde{U}} = M_{\widetilde{D}} = M_{\widetilde{Q}}$, and $\sqrt{s}$ always keeping the other parameters fixed at their reference values and choosing $m_{h^0} = 60$, 80, and 100 GeV. Whenever a curve has two branches then the lower one refers to $\tan\beta < 1$ and its endpoint to $\tan\beta = 0.5$. Whenever there is only a single branch then $\tan\beta > 1$. We choose $M_{\widetilde{U}}$, $M_{\widetilde{D}}$, and $M_{\widetilde{Q}}$ larger than $\sqrt{s}/2$ to avoid sfermion pair production; as mentioned in Sec. 1, we focus attention on indirect SUSY signals. We observe that $2\,\mathcal{R}e\,\Delta_{\widetilde{Q}}$ is always negative. From Figs. 3

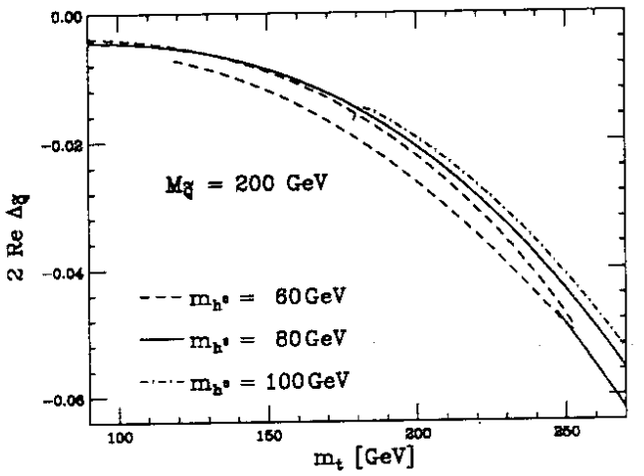

Fig. 3. One-loop radiative corrections to $\sigma(e^+e^- \to Zh^0)$ at $\sqrt{s} =$ 300 GeV due to three generations of squarks and sleptons as a function of m_t for three choices of m_{h^0} assuming $A_U = A_D = M_{\tilde{U}} = M_{\tilde{D}} = M_{\tilde{Q}} = 200$ GeV

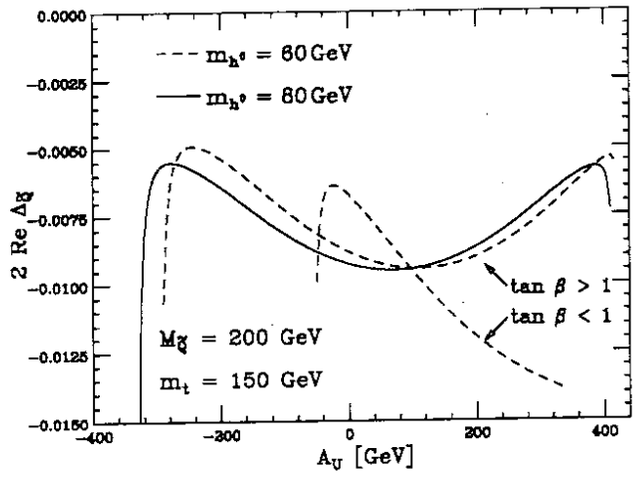

Fig. 4. One-loop radiative corrections to $\sigma(e^+e^- \to Zh^0)$ at $\sqrt{s} =$ 300 GeV due to three generations of squarks and sleptons as a function of $A_U = A_D$ for three choices of m_{h^0} assuming $m_t =$ 150 GeV and $M_{\tilde{U}} = M_{\tilde{D}} = M_{\tilde{Q}} = 200$ GeV

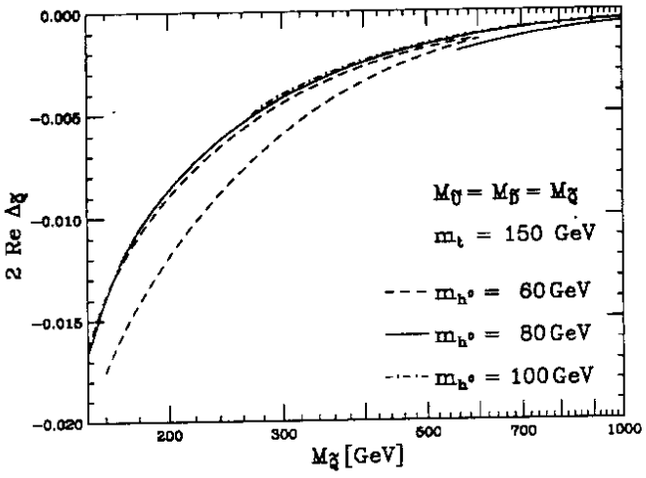

Fig. 5. One-loop radiative corrections to $\sigma(e^+e^- \to Zh^0)$ at $\sqrt{s} =$ 300 GeV due to three generations of squarks and sleptons as a function of $M_{\tilde{U}} = M_{\tilde{D}} = M_{\tilde{Q}}$ for three choices of m_{h^0} assuming $m_t = 150$ GeV and $A_U = A_D = 200$ GeV

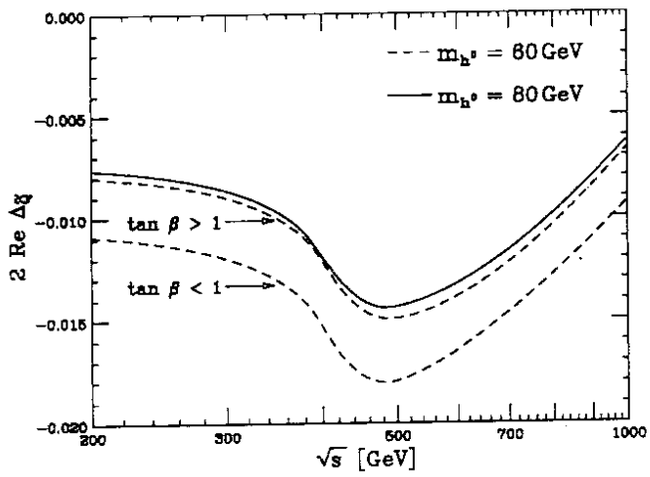

Fig. 6. One-loop radiative corrections to $\sigma(e^+e^- \to Zh^0)$ due to three generations of squarks and sleptons as a function of $\sqrt{s}$ for three choices of m_{h^0} assuming $m_t = 150$ GeV and $A_U = A_D = M_{\tilde{U}} = M_{\tilde{D}} = M_{\tilde{Q}} = 200$ GeV

and 5 we see that the magnitude of the sfermionic corrections increases with increasing m_t and decreasing $M_{\tilde{Q}}$ and remains typically below 5%. Figure 4 tells us that the corrections are independent of A_U, except towards to edges of the allowed parameter space, where they may become quite large. In Fig. 6 we see that the corrections vary only feebly with energy; the dents around $\sqrt{s} = 400$ GeV are due to the open-flavour thresholds of the sfermions.

To obtain the full sfermionic corrections to $\sigma(e^+e^- \to Zh^0)$ in the MOMS scheme, we need to also include the corresponding contribution from Δr; see (2.9). In Figs. 7–9, we study the dependence of $\Delta r_{\tilde{Q}}$ on m_t, $A_U = A_D$, and $M_{\tilde{U}} = M_{\tilde{D}} = M_{\tilde{Q}}$ in a similar fashion as this is done for $2\mathcal{R}e\,\Delta_{\tilde{Q}}$ in Figs. 3–5. Again, the contributions are negative throughout. However, since $\Delta r_{\tilde{Q}}$ enters (2.9) with a minus sign, the overall sfermionic correction is appreciably reduced when the Born result is parameterized in terms of G_F as is the case in (2.9).

Of course, the study of the sfermionic contributions to Δr is interesting in its own right. It is well known that the fine-tuning of Δr so that the theoretical prediction of the muon lifetime agrees with its precisely measured value establishes a relation between the known and the unknown masses of the theory; for a very recent review of Δr in the SM see [23]. Since m_Z has been measured quite accurately and the influence of the Higgs sector is screened [24], Δr mainly governs the M_W–m_t interdependence. Assuming m_t to be known, a small additional contribution, $\delta\Delta r$, to Δr shifts the predicted value of m_W by approximately

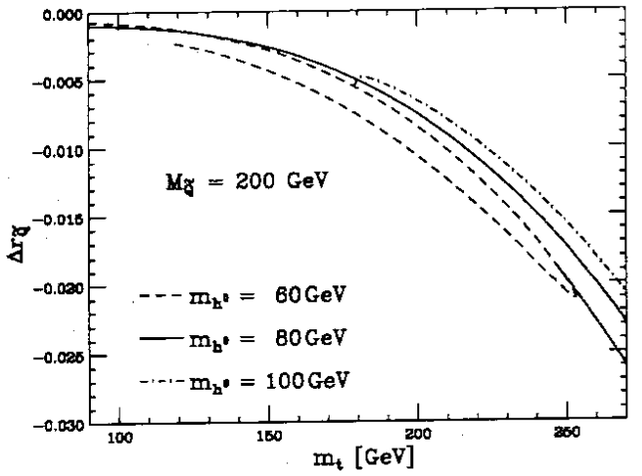

Fig. 7. One-loop radiative corrections to Δr due to three generations of squarks and sleptons as a function of m_t for three choices of m_{h^0} assuming $A_U = A_D = M_{\widetilde{U}} = M_{\widetilde{D}} = M_{\widetilde{Q}} = 200$ GeV

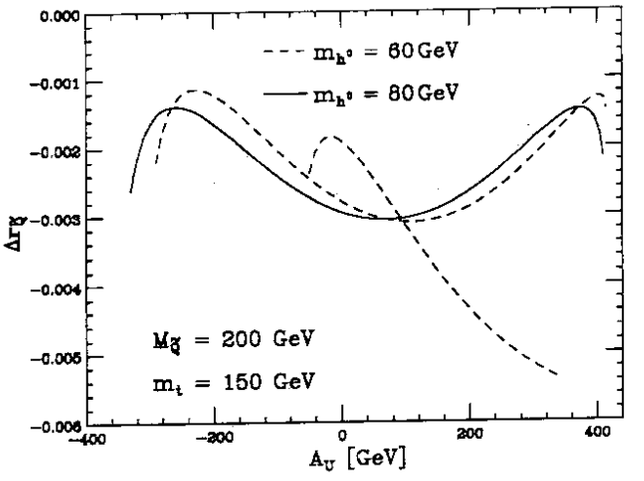

Fig. 8. One-loop radiative corrections to Δr due to three generations of squarks and sleptons as a function of $A_U = A_D$ for three choices of m_{h^0} assuming $m_t = 150$ GeV and $M_{\widetilde{U}} = M_{\widetilde{D}} = M_{\widetilde{Q}} = 200$ GeV

$$\delta m_W = -\frac{s_w^2 m_W}{2\,(c_w^2 - s_w^2)\,(1-\Delta r)}\,\delta\Delta r \approx -170\ \text{MeV} \times [\delta\Delta r \text{ in } \%]\,. \tag{3.2}$$

Vice versa, keeping m_W fixed, the prediction of m_t is shifted by

$$\delta m_t = \frac{4\pi^2\sqrt{2}s_w^2}{3G_F c_w^2 m_t}\,\delta\Delta r \approx 30\ \text{GeV} \times \left[\frac{150\ \text{GeV}}{m_t}\right] \times [\delta\Delta r \text{ in } \%]\,. \tag{3.3}$$

Thus, we read from Figs. 7–9 that in the presence of sfermions higher values of m_W and/or smaller values of m_t are favoured by the Δr analysis. The effect may be quite significant for large m_t and small $M_{\widetilde{U}}$, $M_{\widetilde{D}}$, and $M_{\widetilde{Q}}$, especially if $\tan\beta < 1$; see Figs. 7 and 9, respectively. Similarly to Fig. 4, the dependence on A_U and A_D is weak; see Fig. 8. In the future, after more precise m_W measurements and the discovery of the top quark, this type of analysis could be used to raise the lower bounds on the sfermion masses.

Having studied $2\,\mathcal{R}e\,\Delta_{\widetilde{Q}}$ and $\Delta r_{\widetilde{Q}}$ separately, we are now in a position to present the combined sfermionic corrections to $\sigma(e^+e^- \to Zh^0)$ including the resummation of the leading logarithms of the MSSM; see (2.9). In Fig. 10, we show these corrections relative to the SM prediction at $\sqrt{s} = 300$ GeV as a function of m_{h^0} for $A_U = A_D = M_{\widetilde{U}} = M_{\widetilde{D}} = M_{\widetilde{Q}} = 150$, 300, and 450 GeV assuming $m_t = 150$ GeV. In the calculation of $\sin^2(\beta-\alpha)_{\rm LL}$ we set $m_{A^0} = 200$ GeV. We allow for values of m_{h^0} below the experimental lower bound at 60 GeV to visualize how the branches of $\tan\beta < 1$ and $\tan\beta > 1$ are connected. As expected from Figs. 3–9 in connection with (2.9), a partial cancellation is at work between $2\,\mathcal{R}e\,\Delta_{\widetilde{Q}}$ and $\Delta r_{\widetilde{Q}}$, which enters (2.9) with a prefactor of -2. We see that the overall effect is negative and below 2% for $M_{\widetilde{Q}} > 150$ GeV, which we impose to avoid sfermion production.

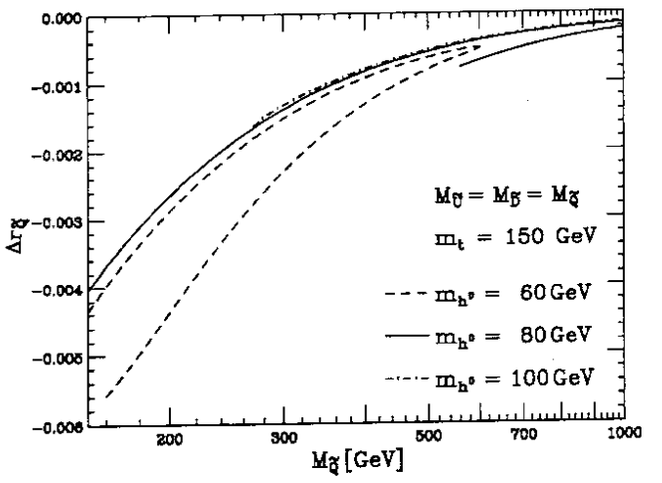

Fig. 9. One-loop radiative corrections to Δr due to three generations of squarks and sleptons as a function of $M_{\widetilde{U}} = M_{\widetilde{D}} = M_{\widetilde{Q}}$ for three choices of m_{h^0} assuming $m_t = 150$ GeV and $A_U = A_D = 200$ GeV

Experimental verification of the effects shown in Fig. 10 requires precise knowledge of the absolute luminosity and will be extremely difficult to achieve. However, uncertainties in the luminosity calibration may be largely eliminated by forming ratios of cross sections. In Sec. 2, we have proposed to consider the quantity $R = \sigma(e^+e^- \to Zh^0)/\sigma(e^+e^- \to \mu^+\mu^-)$. Apart from experimental advantages, this quantity is more sensitive to MSSM effects, since Δr essentially drops out, so that the above-mentioned cancellation is set off. On the other hand, the sfermionic corrections to $\sigma(e^+e^- \to \mu^+\mu^-)$ (in the OMS scheme) are very small, of the order of a few tenths of a percent. As a consequence, R essentially probes the combination $\sin^2(\beta-\alpha)_{\rm LL} + 2\,\mathcal{R}e\,\Delta_{\widetilde{Q}}$; see (2.9). In Fig. 11, we show the variation of R, $\Delta R_{\widetilde{Q}}$, normalized to the SM prediction, $R_{\rm SM}$, in a similar fashion as we have done this for $\sigma(e^+e^- \to Zh^0)$ in Fig. 10.

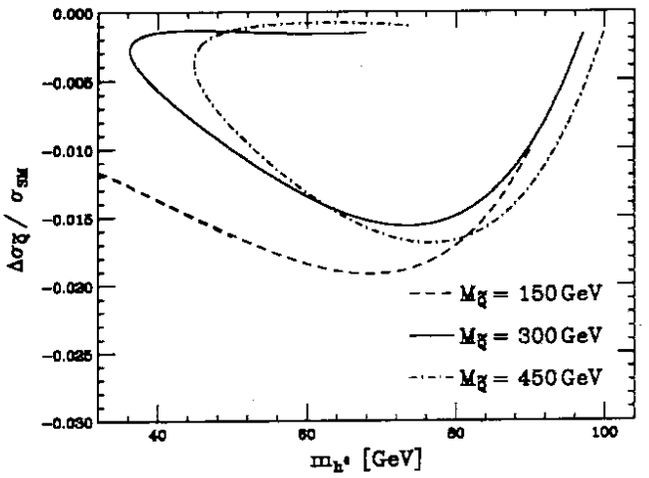

Fig. 10. Relative deviation of the MSSM prediction of $\sigma(e^+e^- \to Zh^0)$ from its SM value at $\sqrt{s} = 300$ GeV as a function of m_{h^0} for three choices of $A_U = A_D = M_{\widetilde{U}} = M_{\widetilde{D}} = M_{\widetilde{Q}}$ assuming $m_t = 150$ GeV. This includes all leading-log corrections with $m_{A^0} = 200$ GeV as well as the sfermionic one-loop contributions

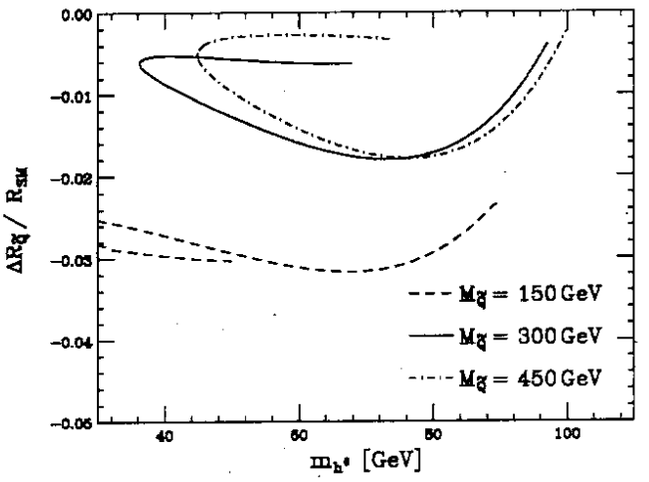

Fig. 11. Relative deviation of the MSSM prediction of $\sigma(e^+e^- \to Zh^0)/\sigma(e^+e^- \to \mu^+\mu^-)$ from its SM value at $\sqrt{s} = 300$ GeV as a function of m_{h^0} for three choices of $A_U = A_D = M_{\widetilde{U}} = M_{\widetilde{D}} = M_{\widetilde{Q}}$ assuming $m_t = 150$ GeV. This includes all leading-log corrections with $m_{A^0} = 200$ GeV as well as the sfermionic one-loop contributions

The corrections are negative in the allowed m_{h^0} range and their magnitude does not exceed 3% for our typical choices of parameters.

In the remainder of this section, we consider γh^0 associated production through the decay of real Z bosons. The partial width of this channel can be accurately predicted in the SM [25]. Figure 12 displays the sfermion-induced shift in $\Gamma(Z \to \gamma h^0)$, $\Delta\Gamma_{\widetilde{Q}}$, relative to the SM prediction, $\Gamma_{\rm SM}$, as a function of m_{h^0} for $A_U = A_D = M_{\widetilde{U}} = M_{\widetilde{D}} = M_{\widetilde{Q}} = 100$, 150, 200, and 300 GeV assuming $m_t = 150$ GeV and $\mu = 100$ GeV. With this choice of parameters the effect amounts to at most 4% in the window $m_{h^0} \gtrsim 60$ GeV. We point out that the effect may be increased by choosing the mass of the right-handed stop to be close to $m_Z/2$. However,

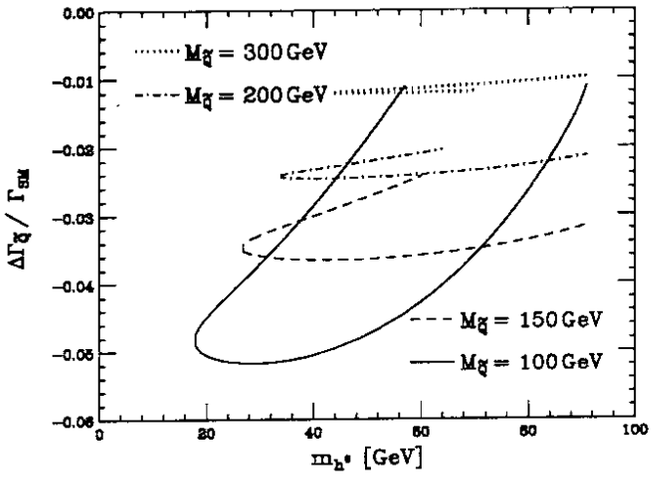

Fig. 12. Relative deviation of $\Gamma(Z \to \gamma h^0)$ from its SM value in the presence of three generations of squarks and sleptons as a function of m_{h^0} for three choices of $A_U = A_D = M_{\widetilde{U}} = M_{\widetilde{D}} = M_{\widetilde{Q}}$ assuming $m_t = 150$ GeV and $\mu = 100$ GeV

the corrections will never be large enough to render this process relevant for Higgs hunting at LEP and SLC. We note in passing that, apart from typographical errors in Table B.1 of [7], our results for the sfermionic corrections to $Z \to \gamma h^0$ agree with [7], where similar conclusions regarding the sfermionic sector were obtained.

4. Conclusions

We have looked for indirect signals for supersymmetry in a scenario where the superpartners and the second Higgs doublet are kinematically unaccessible. In this scenario the lightest CP-even scalar, h^0, has similar couplings to the gauge bosons and matter fields as the standard-model Higgs boson. For large m_t the dominant loop effects are expected to arise from the sfermion sector due to the enhanced couplings of the Higgs-boson to the top squarks.

The Zh^0 associated production in e^+e^- annihilation is one of the most promising candidates to reveal such deviations from the standard-model predictions. We have calculated the sfermionic corrections at one loop to the cross sections of this process and of $e^+e^- \to \mu^+\mu^-$. We have found that the corrections to the ratio are always negative and that their magnitude grows as m_t^2. For $m_t = 150$ GeV they are typically of the order of a few percent for sfermion masses in the 200–300 GeV range. On the other hand, heavy sfermions decouple. In conclusion, sfermionic corrections will act in the same direction as the tree-level suppression factor $\sin^2(\beta - \alpha)$ and thus improve the prospects of detecting a deviation from the standard model.

Acknowledgement. Both of us would like to thank Howard Haber for very useful discussions at the initial stage of this work.

Appendix A: Feynman rules for the squark sector

In this appendix we summarize the sfermion mass matrices and interaction matrices. The mass matrices

for the squarks and sleptons [$\widetilde{Q} \equiv (\widetilde{U}_L, \widetilde{D}_L)$, $\widetilde{D} \equiv \widetilde{D}^*_R$ and $\widetilde{U} \equiv \widetilde{U}^*_R$; generation labels will be suppressed] are expressed in terms of the soft SUSY mass parameters

$$\mathcal{V}^{\widetilde{Q}}_{\rm mass} = M^2_{\widetilde{Q}} \widetilde{Q}^\dagger \widetilde{Q} + M^2_{\widetilde{U}} \widetilde{U}^* \widetilde{U} + M^2_{\widetilde{D}} \widetilde{D}^* \widetilde{D} \qquad (A.1)$$

and trilinear Higgs-sfermion-sfermion interactions, which are proportional to the so-called A parameters [26],

$$\mathcal{V}^{\widetilde{Q}}_{\rm int} = -h_U A_U \left(H_2^T \epsilon \widetilde{Q} \right) \widetilde{U} + h_D A_D \left(H_1^T \epsilon \widetilde{Q} \right) \widetilde{D} + \text{h.c.}, \qquad (A.2)$$

where ϵ is the antisymmetric tensor of $\mathrm{SU(2)_L}$. The subscript U (D) corresponds to the up- (down-) type squarks. For the sleptons, the definitions are similar, except that there is no $\widetilde{\nu}_R$. The A-parameters and the squark mass parameters are in general arbitrary 3×3 matrices. Other trilinear terms generated via the F-terms are

$$\mathcal{V}^{\widetilde{Q}}_{\rm F} = -\mu \left[h_U \left(H_1^\dagger \widetilde{Q} \right) \widetilde{U} + h_D \left(H_2^\dagger \widetilde{Q} \right) \widetilde{D} + \text{h.c.} \right], \qquad (A.3)$$

where the Yukawa couplings are related to the masses by

$$h_U = \frac{g m_U}{\sqrt{2} m_W \sin\beta}, \qquad h_D = \frac{g m_D}{\sqrt{2} m_W \cos\beta}, \qquad (A.4))$$

where $g \equiv e/s_{\rm w}$ is the $\mathrm{SU(2)_L}$ gauge coupling. After electroweak symmetry breaking the trilinear terms mix the left-handed and right-handed squark fields. The resulting squared squark mass matrices are listed in Table 1. Here e_Q is the electric charge of the squark $\widetilde{Q}$ (or of the corresponding fermion Q). In our notation: $Q = U, D$; where $U = u, s, t, \nu_e, \nu_\mu, \nu_\tau$ and $D = d, c, b, e, \mu, \tau$ with analogous notation for the squarks. The third component of the isospin $T_3^Q = \frac{1}{2}$ $(-\frac{1}{2})$ for $Q = U$ (D) and the electric charge $e_U = \frac{2}{3}$ (0) for up-type squarks (sleptons) and $e_D = -\frac{1}{3}$ (-1) for down-type squarks (sleptons). The squark mass eigenvalues $M^2_{\widetilde{Q}a}$ $(a = 1, 2)$ and the mixing angle $\theta_{\widetilde{Q}}$ are given by:

$$M^2_{\widetilde{Q}a} = \tfrac{1}{2} \left(\mathrm{tr}\mathcal{M}^2_{\widetilde{Q}} \pm \sqrt{(\mathrm{tr}\mathcal{M}^2_{\widetilde{Q}})^2 - 4\det\mathcal{M}^2_{\widetilde{Q}}} \right),$$

$$\tan 2\theta_{\widetilde{Q}} = \frac{2 \left(\mathcal{M}^2_{\widetilde{Q}} \right)_{12}}{\left(\mathcal{M}^2_{\widetilde{Q}} \right)_{11} - \left(\mathcal{M}^2_{\widetilde{Q}} \right)_{22}}. \qquad (A.5)$$

This definition of the squark mass eigenvalues and mixing angle implies that $M_{\widetilde{Q}1} > M_{\widetilde{Q}2}$ and

$$\mathcal{U}(\theta_{\widetilde{Q}}) \mathcal{M}_{\widetilde{Q}} \mathcal{U}^\dagger(\theta_{\widetilde{Q}}) = \mathrm{diag}(M^2_{\widetilde{Q}1}, M^2_{\widetilde{Q}2}), \qquad (A.6)$$

where the unitary transformation is defined as

$$\mathcal{U}_{ij}(\theta) = \begin{pmatrix} \cos\theta & \sin\theta \\ -\sin\theta & \cos\theta \end{pmatrix}. \qquad (A.7)$$

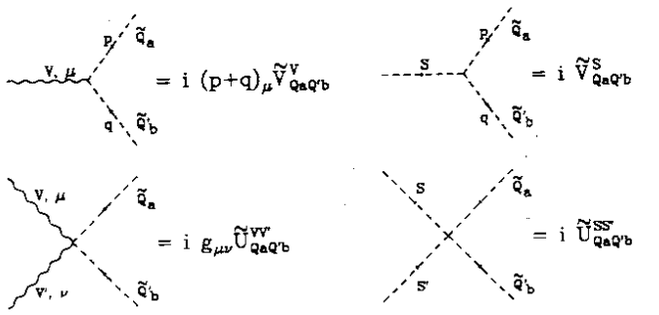

Fig. 12. Feynman rules for trilinear and quartic couplings of a squark pair to Higgs and gauge bosons

The trilinear and quartic couplings of a squark pair to one and two Higgs bosons and gauge bosons are summarized in Table 1 with the vertices defined as in Fig. 2 [3,27]. Note that the subscript $Q' = Q$ in those vertices where $V = Z, \gamma$ and can therefore be suppressed. The vertices for the squark mass eigenstates can be obtained by rotating the interaction matrices involving the electroweak eigenstates (summation over twice occurring indices is assumed)

$$\widetilde{V}^W_{UaDb} = \mathcal{U}_{ac}(\theta_{\widetilde{U}}) \widetilde{\mathcal{V}}^W_{UcDd} \mathcal{U}^\dagger_{db}(\theta_{\widetilde{D}}),$$
$$\widetilde{V}_{Qab} = \mathcal{U}_{ac}(\theta_{\widetilde{Q}}) \widetilde{\mathcal{V}}_{Qcd} \mathcal{U}^\dagger_{db}(\theta_{\widetilde{Q}}). \qquad (A.8)$$

Here the interaction matrices for the electroweak squark eigenstates $\widetilde{\mathcal{V}} = \widetilde{\mathcal{V}}^V, \widetilde{\mathcal{U}}^{VV'}, \widetilde{\mathcal{U}}^{WW}, \widetilde{\mathcal{V}}^{h_i}, \widetilde{\mathcal{U}}^{h_i h_j}$ are given by

$$\widetilde{\mathcal{V}}^W_{UaDb} = -\frac{g}{\sqrt{2}} \mathrm{diag}\,(1, 0),$$

$$\widetilde{\mathcal{V}}^\gamma_{Qab} = -e e_Q \,\mathrm{diag}\,(1, 1),$$

$$\widetilde{\mathcal{V}}^Z_{Qab} = -\frac{g}{c_{\rm w}} \mathrm{diag} \left(T_3^Q - e_Q s^2_{\rm w}, -e_Q s^2_{\rm w} \right), \qquad (A.9)$$

$$\widetilde{\mathcal{U}}^{WW}_{Qab} = \frac{g^2}{2} \mathrm{diag}\,(1, 0),$$

$$\widetilde{\mathcal{U}}^{V_i V_j}_{Qac} = 2 \widetilde{\mathcal{V}}^{V_i}_{Qab} \widetilde{\mathcal{V}}^{V_j}_{Qbc} \qquad V_i = Z, \gamma.$$

Appendix B: One-loop corrections to $e^+e^- \to V h_i$

Here we present the calculation of the Feynman diagrams. We have done all the calculations in dimensional regularization ($n = 2\omega$). The results are presented in terms of the following integrals:

Table 1. The squark mass matrices and interaction matrices with Higgs bosons and gauge bosons

$$\mathcal{M}^2_{\tilde{U}} = \begin{bmatrix} M^2_{\tilde{Q}} + m_U^2 + m_Z^2(T_3^U - e_U s_w^2)\cos 2\beta & m_U(A_U - \mu\cot\beta) \\ m_U(A_U - \mu\cot\beta) & M^2_{\tilde{U}} + m_U^2 + m_Z^2 e_U s_w^2 \cos 2\beta \end{bmatrix}$$

$$\mathcal{M}^2_{\tilde{D}} = \begin{bmatrix} M^2_{\tilde{Q}} + m_D^2 + m_Z^2(T_3^D - e_D s_w^2)\cos 2\beta & m_D(A_D - \mu\tan\beta) \\ m_D(A_D - \mu\tan\beta) & M^2_{\tilde{D}} + m_D^2 + m_Z^2 e_D s_w^2 \cos 2\beta \end{bmatrix}$$

$$\mathcal{U}^{H^0H^0}_{Uab} = -\frac{g^2}{2m_W^2}\mathrm{diag}\left[\sin^2\alpha\, m_U^2/\sin^2\beta + \cos 2\alpha(T_3^U - e_U s_w^2)m_Z^2\,,\ \sin^2\alpha\, m_U^2/\sin^2\beta + \cos 2\alpha\, e_U s_w^2 m_Z^2\right]$$

$$\mathcal{U}^{h^0h^0}_{Uab} = -\frac{g^2}{2m_W^2}\mathrm{diag}\left[\cos\alpha^2\, m_U^2/\sin^2\beta - \cos 2\alpha(T_3^U - e_U s_w^2)m_Z^2\,,\ \cos\alpha^2\, m_U^2/\sin^2\beta - \cos 2\alpha\, e_U s_w^2 m_Z^2\right]$$

$$\mathcal{U}^{H^0h^0}_{Uab} = -\frac{g^2\sin 2\alpha}{4m_W^2}\mathrm{diag}\left[m_U^2/\sin^2\beta - 2(T_3^U - e_U s_w^2)m_Z^2\,,\ m_U^2/\sin^2\beta - 2e_U s_w^2 m_Z^2\right]$$

$$\mathcal{U}^{H^0H^0}_{Dab} = -\frac{g^2}{2m_W^2}\mathrm{diag}\left[\cos\alpha^2\, m_D^2/\cos^2\beta - \cos 2\alpha(T_3^D - e_D s_w^2)m_Z^2\,,\ \cos\alpha^2 m_D^2/\cos^2\beta - \cos 2\alpha\, e_D s_w^2 m_Z^2\right]$$

$$\mathcal{U}^{h^0h^0}_{Dab} = -\frac{g^2}{2m_W^2}\mathrm{diag}\left[\sin^2\alpha m_D^2/\cos^2\beta + \cos 2\alpha(T_3^D - e_D s_w^2)m_Z^2\,,\ \sin^2\alpha m_D^2/\cos^2\beta + \cos 2\alpha\, e_D s_w^2 m_Z^2\right]$$

$$\mathcal{U}^{H^0h^0}_{Dab} = -\frac{g^2\sin 2\alpha}{4m_W^2}\mathrm{diag}\left[-m_D^2/\cos^2\beta - 2(T_3^D - e_D s_w^2)m_Z^2\,,\ -m_D^2/\cos^2\beta - 2e_D s_w^2 m_Z^2\right]$$

$$\tilde{\mathcal{V}}^{H^0}_{Uab} = -\frac{g}{m_W}\begin{bmatrix} \sin\alpha\, m_U^2/\sin\beta + \cos(\alpha+\beta)(T_3^U - e_U s_w^2)m_Z^2 & \frac{1}{2}m_U(-\mu\cos\alpha + A_U\sin\alpha)/\sin\beta \\ \frac{1}{2}m_U(-\mu\cos\alpha + A_U\sin\alpha)/\sin\beta & \sin\alpha\, m_U^2/\sin\beta + \cos(\alpha+\beta)e_U s_w^2 m_Z^2 \end{bmatrix}$$

$$\tilde{\mathcal{V}}^{h^0}_{Uab} = -\frac{g}{m_W}\begin{bmatrix} \cos\alpha\, m_U^2/\sin\beta - \sin(\alpha+\beta)(T_3^U - e_U s_w^2)m_Z^2 & \frac{1}{2}m_U(A_U\cos\alpha + \mu\sin\alpha)/\sin\beta \\ \frac{1}{2}m_U(A_U\cos\alpha + \mu\sin\alpha)/\sin\beta & \cos\alpha\, m_U^2/\sin\beta - \sin(\alpha+\beta)e_U s_w^2 m_Z^2 \end{bmatrix}$$

$$\tilde{\mathcal{V}}^{H^0}_{Dab} = -\frac{g}{m_W}\begin{bmatrix} \cos\alpha\, m_D^2/\cos\beta + \cos(\alpha+\beta)(T_3^D - e_D s_w^2)m_Z^2 & \frac{1}{2}m_D(-\mu\sin\alpha + A_D\cos\alpha)/\cos\beta \\ \frac{1}{2}m_D(-\mu\sin\alpha + A_D\cos\alpha)/\cos\beta & \cos\alpha\, m_D^2/\cos\beta + \cos(\alpha+\beta)e_D s_w^2 m_Z^2 \end{bmatrix}$$

$$\tilde{\mathcal{V}}^{h^0}_{Dab} = -\frac{g}{m_W}\begin{bmatrix} -\sin\alpha\, m_D^2/\cos\beta - \sin(\alpha+\beta)(T_3^D - e_D s_w^2)m_Z^2 & -\frac{1}{2}m_D(A_D\sin\alpha + \mu\cos\alpha)/\cos\beta \\ -\frac{1}{2}m_D(A_D\sin\alpha + \mu\cos\alpha)/\cos\beta & -\sin\alpha\, m_D^2/\cos\beta - \sin(\alpha+\beta)e_D s_w^2 m_Z^2 \end{bmatrix}$$

$$A_0(m^2) = -16\pi^2 i\int\frac{\mathrm{d}^{2\omega}k}{(2\pi)^{2\omega}}\frac{1}{k^2 - m_1^2 + i\epsilon}\,,$$

$$\{B_0; B_\mu; B_{\mu\nu}\}(p^2, m_1^2, m_2^2) =$$

$$-16\pi^2 i\int\frac{\mathrm{d}^{2\omega}k}{(2\pi)^{2\omega}}\frac{\{1; k_\mu; k_\mu k_\nu\}}{(k^2 - m_1^2 + i\epsilon)[(k+p)^2 - m_2^2 + i\epsilon]}\,,$$

$$\{C_0; C_\mu; C_{\mu\nu}\}(p^2, q^2, (p+q)^2, m_1^2, m_2^2, m_3^2) =$$

$$-16\pi^2 i\int\frac{\mathrm{d}^{2\omega}k}{(2\pi)^{2\omega}}\frac{\{1; k_\mu; k_\mu k_\nu\}}{(k^2 - m_1^2 + i\epsilon)[(k+p)^2 - m_2^2 + i\epsilon]} \times\frac{1}{[(k+p+q)^2 - m_2^2 + i\epsilon]}\,, \qquad (B.1)$$

$$\begin{aligned} B_\mu &= p_\mu B_1\,,\\ B_{\mu\nu} &= p_\mu p_\nu B_{21} + g_{\mu\nu}B_{22}\,,\\ C_\mu &= p_\mu C_{11} + q_\mu C_{12}\,,\\ C_{\mu\nu} &= p_\mu p_\nu C_{21} + k_\mu k_\nu C_{22}\\ &\quad + (p_\mu k_\nu + k_\mu p_\nu)C_{23} + g_{\mu\nu}C_{24}\,. \end{aligned} \qquad (B.2)$$

Furthermore, it is convenient to define

$$B_{22}(q^2, m_1^2, m_2^2) = 4B_{22}(q^2, m_1^2, m_2^2) - A_0(m_1^2) - A_0(m_2^2)\,, \qquad (B.3)$$

in conjunction with the decompositions

The relevant vertex corrections and self-energies are

$$A_{WW}(q^2) = \frac{1}{16\pi^2} \sum_{a,b} N_c \left| \tilde{V}^W_{UaDb} \right|^2 B_{22}(q^2, M^2_{\tilde{Q}a}, M^2_{\tilde{Q}b}),$$

$$A_{VV'}(q^2) = \frac{1}{16\pi^2} \sum_{Q,a,b} N_c \tilde{V}^V_{Qab} \tilde{V}^{V'}_{Qab} B_{22}(q^2, M^2_{\tilde{Q}a}, M^2_{\tilde{Q}b}),$$

$$A_{h_i h_j}(q^2) = -\frac{1}{16\pi^2} \sum_{Q,a,b} N_c \tilde{V}^{h_i}_{Qab} \tilde{V}^{h_j}_{Qba} B_0(q^2, M^2_{\tilde{Q}a}, M^2_{\tilde{Q}b}) + \frac{1}{16\pi^2} \sum_{Q,a} N_c \tilde{U}^{h_i h_j}_{Qaa} A_0(M^2_{\tilde{Q}a}),$$

$$\Gamma^1_{VV'h_i} = -\frac{1}{8\pi^2} \sum_{Q,a,b,c} N_c \tilde{V}^V_{Qab} \tilde{V}^{h_i}_{Qbc} \tilde{V}^{V'}_{Qca} \times \left[4C_{24} - B_0(m^2_{h_i}, M^2_{\tilde{Q}b}, M^2_{\tilde{Q}c}) \right],$$

$$\Gamma^4_{VV'h_i} = \frac{1}{2\pi^2} \sum_{Q,a,b,c} N_c \tilde{V}^V_{Qab} \tilde{V}^{h_i}_{Qbc} \tilde{V}^{V'}_{Qca} (C_{23} - C_{22}), \quad (B.4)$$

where we abbreviate $\Gamma = \Gamma(q^2_V, q^2_{h^0}, q^2_{V'})$ and $C = C(q^2_V, q^2_{h^0}, q^2_{V'}, M^2_{\tilde{Q}a}, M^2_{\tilde{Q}b}, M^2_{\tilde{Q}c})$. We recall that the large-m_{A^0} limit considered in this work is implemented by identifying $\alpha = \beta - \pi/2$.

References

1. See, for example, L. Susskind: Phys. Rep. 104 (1984) 181
2. H.P. Nilles: Phys. Rep. 110 (1984) 1; H.E. Haber, G.L. Kane: Phys. Rep. 117 (1985) 75; R. Barbieri: Riv. Nuovo Cimento 11 (1988) 1
3. For a review see e.g.: J.F. Gunion, H.E. Haber, G.L. Kane, S. Dawson: The Higgs Hunter's Guide (Addison-Wesley, Redwood City, 1990)
4. H.E. Haber, R. Hempfling: Phys. Rev. Lett. 66 (1991) 1815; Y. Okada, M. Yamaguchi, T. Yanagida: Prog. Theor. Phys. 85 (1991) 1; J. Ellis, G. Ridolfi, F. Zwirner: Phys. Lett. B257 (1991) 83
5. H.E. Haber, R. Hempfling, Y. Nir: Phys. Rev. D46 (1992) 3015; H.E. Haber, R. Hempfling: UCSC Report SCIPP 91/33 (1992)
6. J. Ellis, G. Ridolfi, F. Zwirner: Phys. Lett. B262 (1992) 477
7. T.J. Weiler, T. Yuan: Nucl. Phys. B318 (1989) 335
8. P.H. Chankowski, S. Pokorski, J. Rosiek: Phys. Lett. B286 (1992) 307; preprint MPI-Ph/92-82 and DFPD/92/TH-48 (1992); D. Pierce, A. Papadopulous: Phys. Rev. D47 (1992) 222
9. R. Hempfling: Ph.D. dissertation, UCSC Report SCIPP 92/28 (1992)
10. A. Sirlin: Phys. Rev. D22 (1980) 971
11. B.A. Kniehl: Nucl. Phys. B352 (1991) 1; Nucl. Phys. B357 (1991) 439; Nucl. Phys. B376 (1992) 3
12. B.A. Kniehl: Z. Phys. C55 (1992) 605
13. G. 't Hooft, M. Veltman: Nucl. Phys. B153 (1979) 365
14. G. Passarino, M. Veltman: Nucl. Phys. B160 (1979) 151
15. C.G. Bollini, J.J. Giambiagi: Phys. Lett. 40B (1972) 566; G. 't Hooft, M. Veltman: Nucl. Phys. B44 (1972) 189
16. W.F.L. Hollik: Fortschr. Phys. 38 (1990) 165
17. J.D. Bjorken: in: Weak Interactions at High Energy and the Production of New Particles: Proceedings of Summer Institute on Particle Physics, 1976, M.C. Zipf (ed.), SLAC Report No. 198 (1976) p. 1
18. B.A. Kniehl: Phys. Lett. B282 (1992) 249
19. R.N. Cahn, M.S. Chanowitz, N. Fleishon: Phys. Lett. 82B (1979) 113
20. K. Hikasa et al. (Particle Data Group): Phys. Rev. D45 (1992) S1
21. L. Rolandi: in: Proceedings of the XXVI International Conference on High Energy Physics, Dallas, Texas, 1992 (to appear)
22. F. Jegerlehner: in: Testing the Standard Model—Proceedings of the 1990 Theoretical Advanced Study Institute in Elementary Particle Physics, Boulder, Colorado, 1990, M. Cvetič, P. Langacker (eds.), (World Scientific, Singapore, 1991) p. 476
23. S. Fanchiotti, B. Kniehl, A. Sirlin: preprint CERN-TH.6749/92 and NYU-Th-92/12/05, Phys. Rev. D (to appear)
24. M. Veltman: Acta. Phys. Pol. B8 (1977) 475; Phys. Lett. 70B (1977) 253
25. M. Spira, A. Djouadi, P.M. Zerwas: Phys. Lett. B276 (1992) 350
26. L. Girardello, M.T. Grisaru: Nucl. Phys. B194 (1982) 65
27. H.E Haber, G.L. Kane: Phys. Rep. 117 (1985) 76

This article was processed using Springer-Verlag TEX Z.Physik C macro package 1.0 and the AMS fonts, developed by the American Mathematical Society.